

# Electron-impurity scattering rate in double layer graphene system at low and high temperature

Digish K. Patel<sup>1</sup>, Mitul J. Patel<sup>1\*</sup>, Bijoy N. Roy<sup>1</sup> and Sagar K. Ambavale<sup>2</sup>

<sup>1</sup>Physics Department, MUIS, Ganpat University, Mehsana, India

<sup>2</sup>Vishwakarma Govt. Engg. College, Chandkheda, Ahmedabad, India  
mjp03@ganpatuniversity.ac.in

Available online at: [www.isca.in](http://www.isca.in), [www.isca.me](http://www.isca.me)

Received 21<sup>st</sup> May 2017, revised 22<sup>nd</sup> July 2017, accepted 1<sup>st</sup> August 2017

## Abstract

Electron-impurity scattering rate ( $\hbar/\tau$ ) is theoretically investigated as a function of quasiparticle energy ( $E_k$ ) for doped Double Layer Graphene System (DLGS) using Boltzmann transport theory at two extreme limits: low and high temperature. Numerically calculated results show that scattering rate ( $\hbar/\tau$ ) of DLGS tends to zero at  $E_k = 0$  in both limits. It is also observed that scattering rate sharply increases with increasing quasi particle energy ( $E_k$ ) to attain a maximum at  $E_k \approx 1.7E_f$  for h-BN,  $E_k \approx 1.3E_f$  for  $Al_2O_3$  and  $E_k \approx 1.2E_f$  for  $HfO_2$ , where  $E_f$  is Fermi energy, and decline thereafter on increasing quasiparticle energy ( $E_k$ ) in low temperature limit. Whereas scattering rate increases nearly linearly with quasiparticle energy ( $E_k$ ) in high temperature limit. In this paper, the role of dielectric environment and interlayer distance between two graphene sheets at low and high temperature limits, on scattering rate has been reported. Carrier mobility is related to scattering rate which can be further controlled by changing interlayer distance, dielectric environment and temperature. The present study of mobility control can be exploited in device designing.

**Keywords:** Electron-impurity scattering rate, Quasiparticle energy, Double Layer Graphene System, Boltzmann transport theory.

## Introduction

Since the experimental realisation of Graphene in 2004, it is playing a dominant role in nano-electronic devices due to its salient features like high mobility, atomic thinness, large surface area and good optical as well as thermal conductivity. According to the studies done by K.S. Novoselov et. al., the experimentally measured value of conductivity ( $\sigma$ ) in monolayer graphene increases linearly with the carrier density ( $n$ ), away from the Diracpoint<sup>1</sup>. This finding is also theoretically confirmed<sup>2-3</sup>. A thorough understanding of the effect on the transport properties due to disorder is always required for making high speed nano-electronic devices. The impact of possible scattering mechanisms (like Coulomb charged impurities, adatoms, vacancies and ripples) on quantum transport property in graphene is investigated by W. Zhu and B.Lv<sup>4</sup>. Their results show that main scattering mechanism in samples with linear behaviour of  $\sigma \propto n$  comes from the Coulomb charged impurities. On the other hand the sub-linear behaviour may result from the remaining other three scattering mechanisms.

Apart from monolayer graphene, other graphene based systems like Bilayer Graphene System (BLGS) and Double Layer Graphene System (DLGS) have been studied experimentally as well as theoretically<sup>5-12</sup>. BLGS is consisting of two graphene layers and are arranged in Bernal stacked (or AB stacked) manner (Figure-1(a)), where three alternate atoms of the upper

graphene sheet lie directly over the center of a hexagon and remaining three atoms lie over an atom in the lower graphene sheet. Whereas in the case of DLGS, the two graphene layers are arranged symmetrically and are separated by dielectric medium having thickness  $d$  (Figure-1(b)). This paper will present the inferences drawn during the studies made over DLGS only. Initially transport properties of DLGS have been studied theoretically as a function of interlayer distance, dielectric environment, carrier density as well as carrier imbalance at zero temperature<sup>11-14</sup>. It is found that the mobility can be improved by controlling these parameters. In the earlier reported results, the calculations were performed for absolute zero temperature, while all the experimental results were obtained at some finite low temperature, other than absolute zero (as experimentally achieving absolute zero is not feasible). In this paper, we will discuss the transport properties of DLGS at two different limits: High and Low temperature, which can be experimentally verified too.

The DLGS has an arrangement of two graphene sheets in AA stacking and these two sheets are separated by distance  $d$ . As can be seen from Figure-1(c), the two spatially separated graphene sheets are immersed in a three-layered homogeneous-mediums with background dielectrics  $\epsilon_1$ ,  $\epsilon_2$ , and  $\epsilon_3$ . In this analysis it is assumed that both the graphene layers are coupled by the Coulomb interaction only. This coulomb interaction exists between the charge impurities and charge carriers. It is further assumed that both the graphene layers have similar

carrier densities. The dielectric function of these layers provides the information regarding the screening effect of scattering potentials due to charged impurities. To investigate the effect of central dielectric layer i.e. the barrier layer, the top layer is assumed to be air and the lowest layer is assumed to be of Aluminum oxide (Al<sub>2</sub>O<sub>3</sub>). In between these two layers, different insulating materials viz. hexagonal Boron nitride (h-BN), Aluminum oxide (Al<sub>2</sub>O<sub>3</sub>) and Hafnium dioxide (HfO<sub>2</sub>) are considered as middle layer.

## Methodology

As per the semi-classical Boltzmann theory, the momentum scattering rate for an electron scattered from the screened Coulomb potential due to disorder is given by<sup>2-3,13-15</sup>

$$\frac{\hbar}{\tau_{ij}} = n_{ij}^{imp} D(E) \int_0^\pi |W_{ij}(q, d, T)|^2 (1 - \cos^2 \theta) d\theta \quad (1)$$

where  $W_{ij}(q, d, T)$  is temperature dependent screened Coulomb potentials given by the following equations<sup>14</sup>;

$$W_{11,22} = (v_{11,22} + (v_{11}v_{22} - v_{12}v_{21})\Pi_{2,1})/\epsilon \quad (2)$$

$$W_{12,21} = v_{12,21}/\epsilon. \quad (3)$$

Temperature dependent static dielectric function ( $\epsilon$ ) for DLGS in equations (2) and (3) is given by<sup>14</sup>;

$$\epsilon(q_1, q_2) = \det(1 - V \Pi) = (1 + v_{11}\Pi_1)(1 + v_{22}\Pi_2) - v_{12}v_{21}\Pi_1\Pi_2 \quad (4)$$

Here  $v_{11,22}$  are the intralayer and  $v_{12,21}$  are interlayer Coulomb interactions, respectively, and are defined as

$$v_{11}(q_1, d) = \frac{4\pi e^2}{q_1} \frac{\epsilon_2 + \epsilon_3 \tanh(q_1 d)}{\epsilon_2(\epsilon_1 + \epsilon_3) + (\epsilon_1^2 + \epsilon_1 \epsilon_3) \tanh(q_1 d)}, \quad (5)$$

$$v_{22}(q_2, d) = \frac{4\pi e^2}{q_2} \frac{\epsilon_2 + \epsilon_1 \tanh(q_2 d)}{\epsilon_2(\epsilon_1 + \epsilon_3) + (\epsilon_1^2 + \epsilon_1 \epsilon_3) \tanh(q_2 d)}, \quad (6)$$

$$v_{12}(q_1, d) = \frac{4\pi e^2}{q_1} \frac{\epsilon_2}{(\epsilon_2(\epsilon_1 + \epsilon_3) + (\epsilon_1^2 + \epsilon_1 \epsilon_3) \tanh(q_1 d)) \cosh(q_1 d)}, \quad (7)$$

And

$$v_{21}(q_2, d) = \frac{4\pi e^2}{q_2} \frac{\epsilon_2}{(\epsilon_2(\epsilon_1 + \epsilon_3) + (\epsilon_1^2 + \epsilon_1 \epsilon_3) \tanh(q_2 d)) \cosh(q_2 d)}. \quad (8)$$

In equation (1),  $\Pi_1(\Pi_2)$  is the temperature dependent static polarization function for upper (lower) graphene layer. The temperature dependent static polarization given as<sup>15</sup>;

$$\Pi_i(q_i, T) = D(k_{fi}) \times \begin{cases} \left[ \frac{\mu_i}{E_{fi}} + \Theta(E_{qi} - 2\mu) \left\{ \frac{\mu_i}{E_{fi}} \left( 1 - \frac{1}{2} \sqrt{1 - \left( \frac{2\mu_i}{E_{qi}} \right)^2} \right) - \frac{E_{qi}}{4\mu_i} \sin^{-1} \left( \frac{2\mu_i}{E_{qi}} \right) \right\} \right]; T \ll T_f \\ \left[ \frac{T}{T_{fi}} \ln 4 + \frac{q_i^2 T_{fi}}{24 k_{fi} T} \right]; T \gg T_f \end{cases} \quad (9)$$

Here  $q_i = 2(E_i/\hbar v_f) \sin(\theta/2)$  is the momentum transferred to a scattered electron. The Fermi wave number on each graphene layer is given as  $k_{fi} = \sqrt{\pi n_{ci}}$  where  $n_{ci}$  is the carrier concentration of  $i^{th}$  graphene layer. In equation (9),  $\mu_i \approx E_f \left[ 1 - \frac{\pi^2}{6} \left( \frac{T}{T_{fi}} \right)^2 \right]$  is the chemical potential at low temperature which is determined by the conservation of the total electron density<sup>10</sup>. Throughout this paper, it is assumed that both layers have identical carrier densities i.e.  $n_{c1} = n_{c2}$ . To ascertain the impact of the middle dielectric layer, it is assumed that the dielectric constants for the top is  $\epsilon_1 = 1$  (for Air) and for the bottom it is  $\epsilon_3 = 12.53$  (for Al<sub>2</sub>O<sub>3</sub>). The three different dielectrics considered as the middle layer, during different cases have dielectric constants as,  $\epsilon_2 = 4$  (for h-BN),  $\epsilon_2 = 12.53$  (for Al<sub>2</sub>O<sub>3</sub>), and  $\epsilon_2 = 22$  (for HfO<sub>2</sub>).

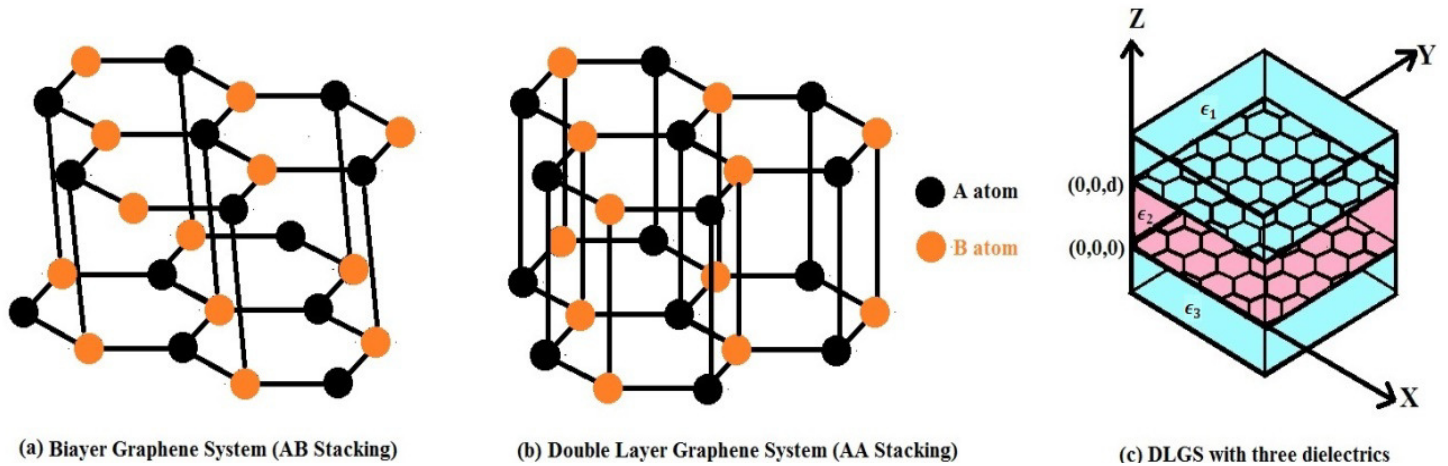


**Figure-1:** (a) Atomic planes arrangement in Bilayer graphene System (BLGS). (b) Atomic planes arrangement in Double Layer Graphene System (DLGS). (c) DLGS immersed in three different dielectrics.

## Results and discussion

The numerical results of equation 1 are calculated as function of different parameters like quasi-particle energy ( $E_k$ ), middle layer dielectric ( $\epsilon_2$ ) and interlayer distance ( $d$ ) at low as well as high temperature limits.

First the normalized scattering rate is calculated as a function of quasi-particle energy at low and high temperature for three different substrates; h-BN,  $\text{Al}_2\text{O}_3$  and  $\text{HfO}_2$ . The variation of normalized scattering rate with quasi-particle energy is shown in Figure-1. Here, the interlayer distance  $d = 1$  nm and total carrier density is  $n_{c1} + n_{c2} = 2 \times 10^{12}/\text{cm}^2$ .

As can be seen from Figure-2, scattering rate ( $\hbar/\tau$ ) of DLGS tends to zero at  $E_k = 0$  in both limits. It is also observed that scattering rate sharply increases with increasing quasiparticle

energy ( $E_k$ ) to attain a maximum at  $E_k \approx 1.7E_f$  for h-BN,  $E_k \approx 1.3E_f$  for  $\text{Al}_2\text{O}_3$  and  $E_k \approx 1.2E_f$  for  $\text{HfO}_2$ , where  $E_f$  is Fermi energy, and decline thereafter on increasing quasiparticle energy ( $E_k$ ) for low temperature limits. Whereas scattering rate increases nearly linearly with quasiparticle energy ( $E_k$ ) in high temperature limit. Scattering rate can be improved by selecting middle layer with low value of dielectrics in both temperature limits.

In order to see the effects of middle layer dielectric  $\epsilon_2$  on scattering rate, the normalized scattering rate is plotted as a function of middle layer dielectric  $\epsilon_2$  for three different bottom layer with dielectric  $\epsilon_3$  as h-BN,  $\text{Al}_2\text{O}_3$  and  $\text{HfO}_2$  at low and high temperature limits as shown in Figure-3. Here, the interlayer distance is  $d = 1$  nm, total carrier density is  $n_{c1} + n_{c2} = 2 \times 10^{12}/\text{cm}^2$  and top dielectric is  $\epsilon_1 = 1$  (Air).

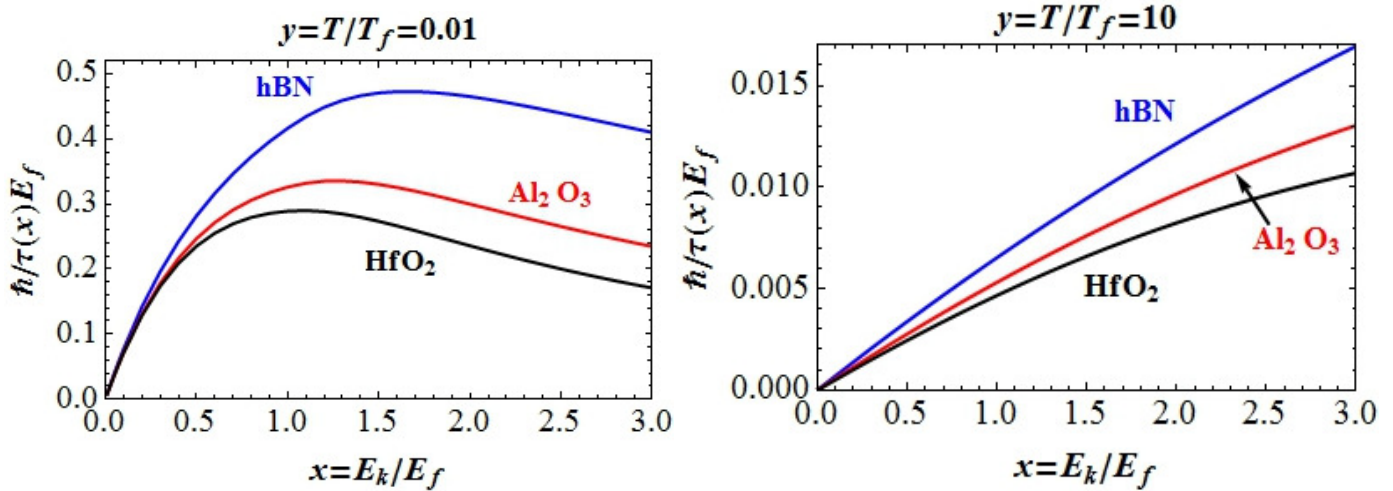


**Figure-2:** Normalized Scattering rate as a function of quasi-particle energy at two extreme limits: low (Left panel) and high (Right panel) temperature for three different substrates; h-BN (Blue),  $\text{Al}_2\text{O}_3$  (Red) and  $\text{HfO}_2$  (Black).

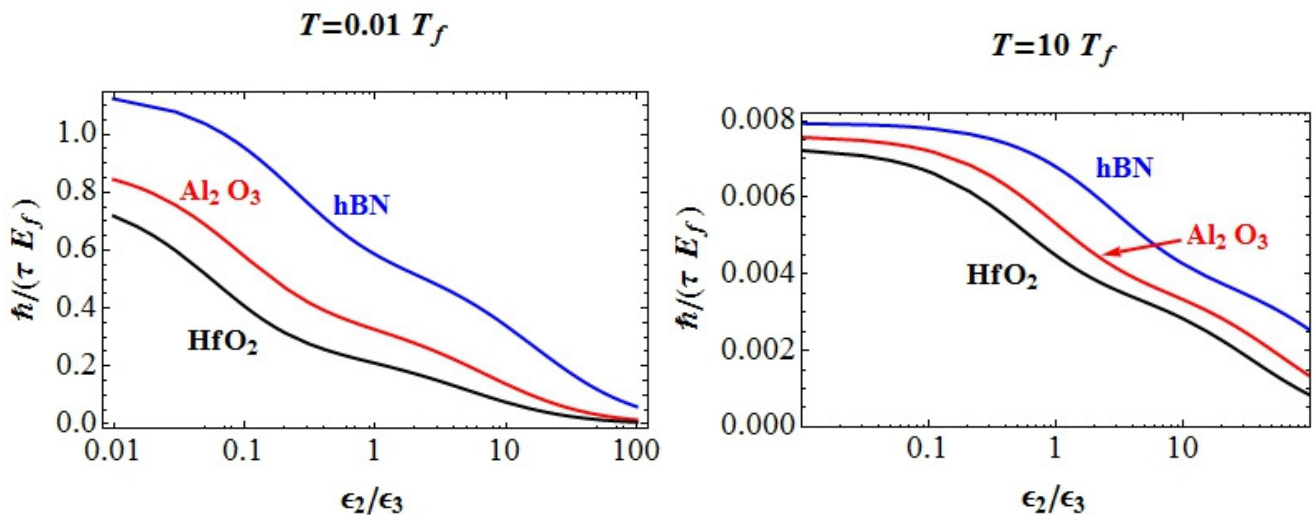


**Figure-3:** Normalized Scattering rate as a function of middle layer dielectric  $\epsilon_2$  at two extreme limits: low (Left panel) and high (Right panel) temperature for three different dielectrics  $\epsilon_3$ ; h-BN (Blue),  $\text{Al}_2\text{O}_3$  (Red) and  $\text{HfO}_2$  (Black).

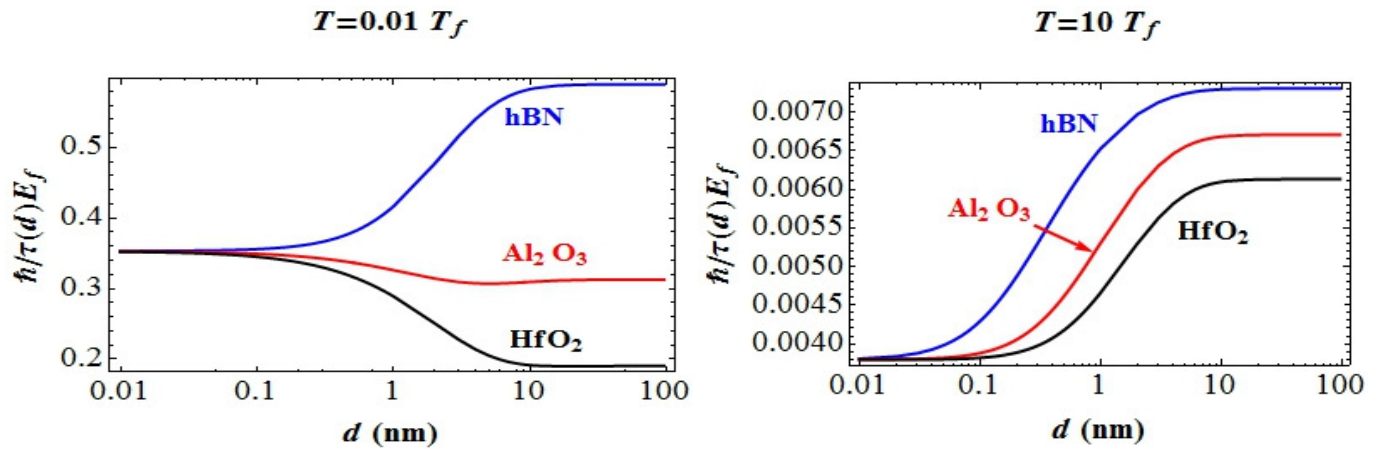


**Figure-4:** Normalized Scattering rate as a function of interlayer distance  $d$  at two extreme limits: low and high temperature for three different substrates; h-BN,  $\text{Al}_2\text{O}_3$  and  $\text{HfO}_2$ . Here, total carrier density is  $n_{c1} + n_{c2} = 2 \times 10^{12}/\text{cm}^2$  and top dielectric is  $\epsilon_1 = 1$  (Air).

The effect of interlayer distance ( $d$ ) (varying from 0.01 nm to 100 nm) on the scattering rate in DLGS structure is also studied. The scattering rate of DGLS as function of  $d$  for three different substrates; h-BN,  $\text{Al}_2\text{O}_3$  and  $\text{HfO}_2$  is plotted in Figure-4. It is found that the scattering rate strongly depends on interlayer distance in the regime  $0.1 \text{ nm} \lesssim d \lesssim 10 \text{ nm}$  while it remains independent with interlayer distance in the regimes  $d \lesssim 0.1 \text{ nm}$  and  $d \gtrsim 10 \text{ nm}$  at both temperature limits. Scattering rate decreases with increasing of interlayer distance for middle dielectrics  $\text{Al}_2\text{O}_3$  and  $\text{HfO}_2$  at low temperature limit. Contrary to this, scattering rate increases with increasing interlayer distance for middle dielectrics  $\text{Al}_2\text{O}_3$  and  $\text{HfO}_2$  at high temperature limit because the intralayer scattering rate  $\hbar/\tau_{11}$  becomes prominent and increases the net scattering rate. In the case of h-BN scattering rate always increases with increasing interlayer distance in both the temperature limits.

## Conclusion

Theoretical investigation of electron impurity scattering rate as a function of different parameters like quasi-particle energy ( $E_k$ ), middle dielectric ( $\epsilon_2$ ) and interlayer distance ( $d$ ) using Boltzmann transport theory has been made at low and high temperature limits. The results suggest that in low temperature limit scattering rate sharply increases with increasing quasi-particle energy ( $E_k$ ) to attain a maximum and decline thereafter but in high temperature limit rate increases nearly linearly with energy. Next at high temperature the scattering rate enhances on increasing interlayer distance from 0.1 nm to 10 nm for all the three middle layer dielectrics h-BN,  $\text{Al}_2\text{O}_3$  and  $\text{HfO}_2$  whereas the nature is not same at low temperature. Further it is found that scattering rate strongly depends on interlayer distance in the regime  $0.1 \text{ nm} \lesssim d \lesssim 10 \text{ nm}$  at both temperature limits. The studies also suggest that mobility (i.e. inverse of scattering rate) in DLGS can be enhanced by filling high dielectric between two graphene layers. The study of electron impurity scattering rate as a function of parameters like quasi-particle energy, middle

dielectric and interlayer distance in DLGS may open a new window to future fabricate graphene-based nano-devices.

## References

1. Novoselov K.S., Geim A.K., Morozov S.V., Jiang D., Zhang Y., Dubonos S.V., Grigorieva I.V. and Firsov A.A. (2004). Electric Field Effect in Atomically Thin Carbon Films. *Science*, 306, 666-669.
2. Hwang E.H., Adam S. and Sarma S.D. (2007). Carrier Transport in Two-Dimensional Graphene Layers. *Phys. Rev. Lett.*, 98, 186806.
3. Noro M., Koshino M. and Ando T. (2010). Theory of Transport in Graphene with Long-Range Scatterers. *J. Phys. Soc. Jpn*, 79, 094713.
4. Zhu W. and Lv B. (2013). Uncovering the Dominant Scattering Mechanism in Graphene System. *Physics Letters A*, 377(25-27), 1649-1654.
5. Ohta T., Bostwick A., Seyller T., Horn K. and Rotenberg E. (2006). Controlling the Electronic Structure of Bilayer Graphene. *Science*, 313, 951-954.
6. Schmidt H., Ludtke T., Barthold P., McCann E., Falko V.I. and Haug R.J. (2008). Tunable Graphene System with Two Decoupled Monolayers. *Appl. Phys. Lett*, 93, 172108.
7. Kim S., Jo I., Nah J., Yao Z., Banerjee S.K. and Tutuc E. (2011). Coulomb Drag of Massless Fermions in Graphene. *Phys. Rev. B*, 83, 161401.
8. Ponomarenko L.A., Geim A.K., Zhukov A.A., Jalil R., Morozov S.V., Novoselov K.S., Grigorieva I.V., Hill E.H., Cheianov V.V., Fal'ko V.I., Watanabe K., Taniguchi T. and Gorbachev R.V. (2011). Tunable Metal-insulator Transition in Double-layer Graphene Heterostructures. *Nature Phys*, 7, 958.
9. Koshino M. (2009). Electronic Transport in Bilayer Graphene. *New Journal of Physics*, 11, 095010.

10. MacDonald A.H., Jung J. and Zhang F. (2012). Pseudospin Order in Monolayer, Bilayer and Double-layer graphene. *Physica Scripta*, T146, 014012.
11. Ponomarenko L.A., Yang R., Mohiuddin T.M., Katsnelson M.I., Novoselov K.S., Morozov S.V., Zhukov A.A., Schedin F., Hill E.W. and Geim A.K. (2009). Effect of a High- $\kappa$  Environment on Charge Carrier Mobility in Graphene. *Phys. Rev. Lett*, 102, 206603.
12. Kechedzhi K., Hwang E.H. and Sarma S.D. (2012). Gate-tunable Quantum Transport in Double-Layer Graphene. *Phys. Rev. B*, 86, 165442.
13. Hosono K. and Wakabayashi K. (2013). Dielectric Environment Effect on Carrier Mobility of Graphene Double-layer Structure. *Appl. Phys. Lett*, 103, 033102.
14. Hosono K. and Wakabayashi K. (2014). Theory of Carrier Transport in Graphene Double-layer Structure with Carrier Imbalance. *Jpn. J. Appl. Phys*, 53, 06JD07.
15. Hwang E.H. and Sarma S.D. (2009). Screening Induced Temperature Dependent Transport in Two Dimensional Graphene. *Phys. Rev. B*, 79, 165404.